A Compact Cryosurgical Apparatus for Minimally Invasive Procedures

YOED RABIN, DSC, THOMAS B. JULIAN, MD, NORMAN WOLMARK, MD

A new liquid-nitrogen–based apparatus for minimally invasive cryosurgery is presented. The cryoprobe was designed for application to breast tumors; however, it can be used for the treatment of other tumors. The cryoprobe has three major components, a cryoneedle, a thermal insulation shell, and a protective tube, which may be assembled as part of the operation. This special assembly keeps destruction to surrounding tissues due to cryoprobe penetration minimal, and allows accurate localization of the cryoprobe tip by means of stereotactic or needle-localization techniques. An alternative cryoprobe consists of a cryoneedle and a thermal insulation shell, which are rigidly connected. The liquid nitrogen supply system has two major components, an air-pressure source and a liquid nitrogen container, which are physically separated. This special configuration allows placement of the liquid nitrogen container adjacent to the cryotreated tissue and decreases the length of the cryoprobe feeding tube. In turn, heat losses to the surroundings are reduced, and therefore coolant consumption is reduced. The short feeding tube allows safe operation at low pressures. The small size of the apparatus makes it attractive for cryosurgical operations. It has been evaluated in gelatin solutions and in porcine skeletal muscle and liver. In-vivo results do not differ significantly from those obtained in gelatin solutions with regard to the dimensions of frozen regions. Using a three cryoprobe configuration, a frozen region with an average diameter of 50 mm and a length of 75 mm was obtained within 11 minutes. The thermal efficiency of that procedure was found to be 43%. (BIOMEDICAL INSTRUMENTATION & TECHNOLOGY 1997; 31:251–258)

Cryosurgery, or the destruction of undesired biologic tissues by freezing, has long been accepted as an important alternative surgical technique.[1–4] Compared with conventional means of destroying tissues, such as surgical excision, radiotherapy, and chemotherapy, visceral cryosurgery (especially when minimally invasive) offers the following potential advantages: substantial decrease in the risk of morbidity, simplicity of the procedure, minimal bleeding, anesthetic effect of low temperatures, shorter period of patient recovery, low cost, minimal scarring, and possible stimulation of the body's immune system.

James Arnott, an English physician, introduced the technique of destruction of biological tissues by freezing in 1865. Since Arnott's first report, numerous cryodevices and techniques have been suggested. These have included precooled metal blocks, precooled needles[5], dry-ice applications, spray/pour freezing with compressed or liquefied gases,[6] refrigeration systems,[7] thermoelectric methods and cryogenic heat pipes,[8] cryoneedles,[9] Joule-Thomsen-effect–based cryoprobes,[10,11] and boiling effect–based cryoprobes.[12–14] However, as a consequence of the extreme cooling power usually needed for cryosurgery, and especially for procedures involving internal organs, the boiling effect has been found by most cryosurgeons to be the preferable cooling technique.

The application of minimally invasive cryosurgery requires the development of a cryoprocedure that minimizes the damage to the surrounding tissues during cryoprobe penetration, utilizing small incisions. Accurate localization of the cryoprobe tip and precise monitoring of the frozen-region formation complete the technique. These criteria have served as the inspiration for continued efforts to reduce cryoprobe diameters and improve techniques such as ultrasonography,[15,16] computed tomography[17] and nuclear magnetic resonance imaging.[18,19] To increase the effectiveness of the cryotreatment, the cooling protocol may be correlated with

Received from the Department of Human Oncology, Allegheny University of the Health Sciences, Pittsburgh, Pennsylvania (YR, TBJ, NW); and the Department of Mechanical Engineering, Carnegie Mellon University, Pittsburgh, Pennsylvania (YR).

Supported in part by Allegheny Singer Research Institute (96-023-1P).

Address correspondence and reprint requests to Dr. Rabin: Department of Mechanical Engineering, Carnegie Mellon University, 5000 Forbes Avenue, Pittsburgh, PA 15213-3890. <e-mail: rabin@ pgh. allegheny.edu>.

The subject matter of this paper was included in a patent application that was filed in the Patent and Trademark Office of the U.S.A. This patent application is patent pending.

criteria for maximal cryodestruction, such as extremely fast cooling,[20,21] low cooling rate at the freezing surface,[22] slow thawing,[23] and repeated cycles of freezing and thawing.[24]

EXPERIMENTAL SETUP

Cryoprobes of two configurations were developed. These devices, which we refer to here as cryoprobes A and B, are illustrated in Figure 1 and 2, respectively. Two types of material were considered for the prototype construction: stainless steel and copper. In general, stainless steel is best suited for surgical tools; however, copper is compatible with the magnetic resonance imaging environment in which these cryoprobes were to be tested. For this reason, copper was used in the initial cryoprobe construction. The advantages in using stainless steel, and its effect on the cryoprobe dimensions are discussed later. All copper tubing used for the experimental cryoprobes in this study had a wall thickness of 0.36 mm. Unless otherwise specified, all tube diameters correspond to the outer diameter (OD).

Cryoprobe A (Figure 1) is constructed of three main components: a cryoneedle (**1**), a thermal insulation shell (**4**), and a protective tube (**6**). The cryoprobe is assembled during and as a part of the cryosurgical procedure, as is described in detail hereafter. The cryoneedle leads the cryofluid forward from feeding tube (**9**) to the cryotreated region and backward to outlet tube (**7**). The cryoneedle has a U-shaped configuration and a sharp pointed tip, which is made of 1.6-mm copper tubing that has an inner diameter (ID) of 0.9 mm (the OD is close to that of a 16-gauge hypodermic needle). The cryoneedles were prepared in lengths between 30 and 150 mm for the present study.

The insulation shell (**4**) has a diameter of 6.4 mm and surrounds a part of the cryoneedle to reduce heat transfer from the surrounding tissues to the cryoneedle. The technique of insulation was planned to be a vacuum; however, it was found experimentally that air insulation is satisfactory for the present application. This can be explained by the fact that the insulation shell was heated to more than 250°C (520°K) at atmospheric pressure during the soldering for sealing. Assuming that air behaves like an ideal gas, the pressure of the air captured in the shell becomes linearly dependent on temperature. Thus, during cryoprobe operation at the boiling temperature of liquid nitrogen (LN_2), i.e. −196°C (77°K), the air pressure drops to less than 15% of a standard atmospheric pressure in the insulation shell, which in turn dramatically decreases its effective thermal conductivity. Protective tube **6** surrounds another part of the cryoneedle, adjacent to the insulation shell but outside the body, to protect the surgeon's hands and to reduce heat transfer from the surroundings to the cryoneedle. Both the insulation shell and the protective tube are free to slide axially along the cryoneedle. Pressurized cryofluid feeds the cryoneedle through tube (**9**) and exits from the cryoneedle through flexible outlet tube (**7**). The only significant heat transfer occurs where the cryoneedle is in direct contact with the tissue, and therefore this area is designated the cryoprobe's active surface. The temperature of the cryoprobe's active surface is monitored by thermocouple (**2**) (Omega TTT-TT-36-36, 0.1 mm in di-

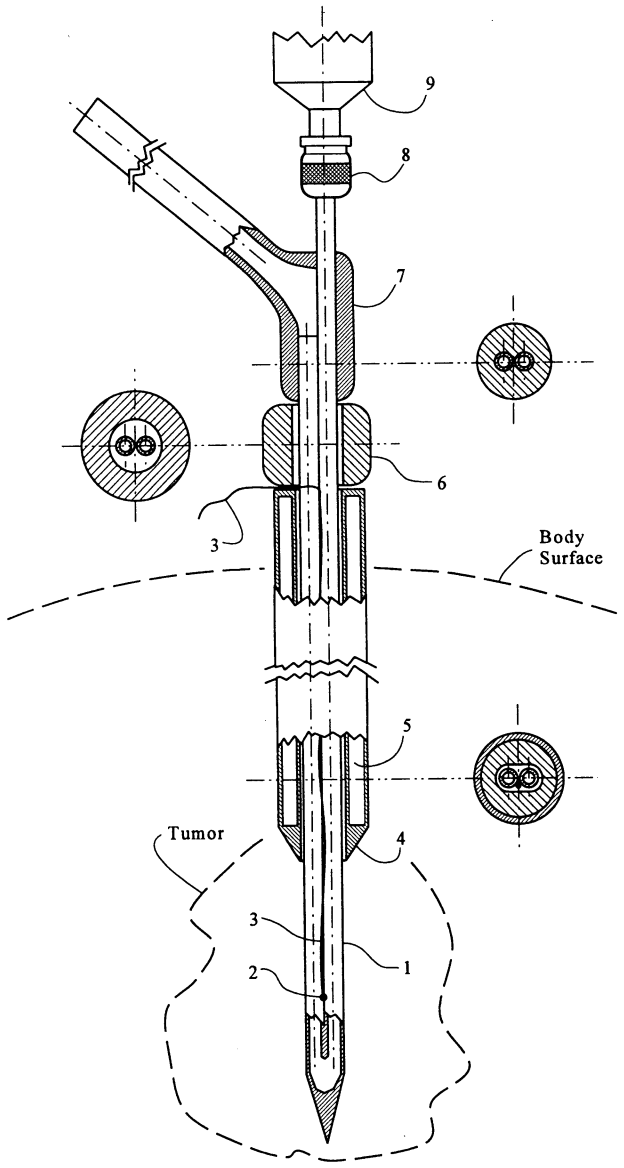

Figure 1. Schematic drawing of cryoprobe A, which is assembled during the localization procedure.

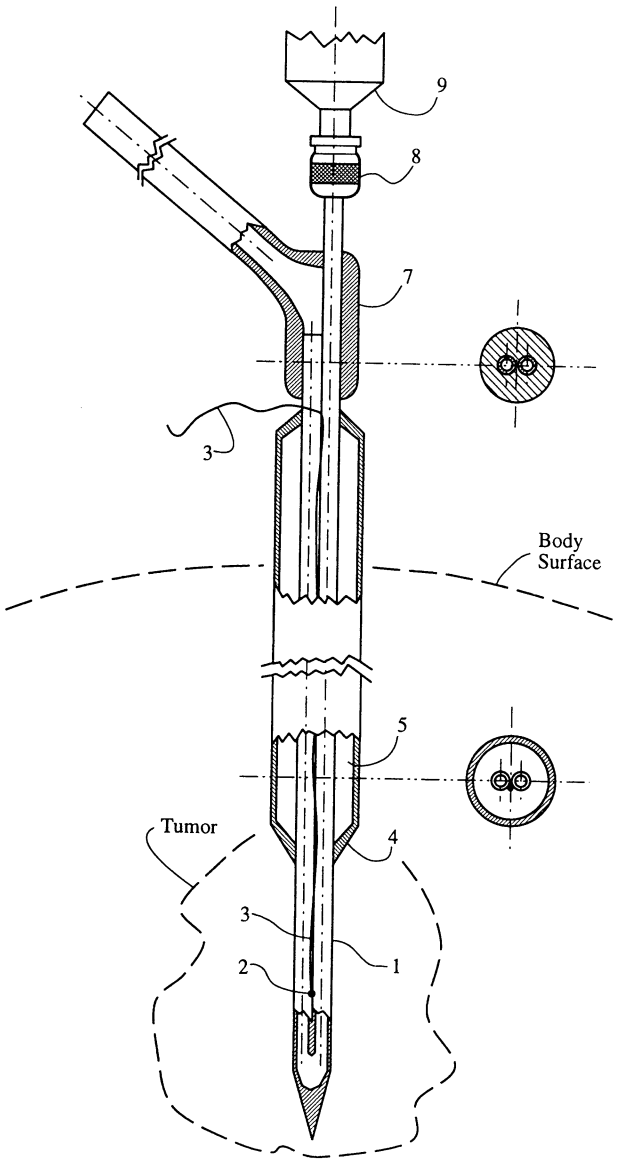

Figure 2. Schematic drawing of cryoprobe B, which is inserted as a single unit into the tissues.

ameter) and its signals are transferred to a temperature-measurement unit **(22)** (Omega HH-23-G1), illustrated in Figure 3.

Cryoprobe A is felt to be most suitable in the application of cryosurgery for breast tumors. This application takes advantage of either stereotactic biopsy or needle-localization techniques. The cryoneedle can be used with a stereotactic device since its dimensions are similar to those of the commonly used biopsy needle. First, the cryoneedle **(1)** is inserted into the center of the tumor (Figure 4a), utilizing a standard biopsy-needle localization technique. After insertion of the cryoneedle to the center of the tumor, a small cut is made in the skin adjacent to the cryoneedle penetration point, on either side of the cryoneedle. Thermal insulation shell **(4)** is then inserted along the cryoneedle (Figure 4b), to an extent that leaves uncovered the desired active surface area extending from the tip of the cryoneedle. Finally, the entire assembly of the cryoprobe is completed (Figure 4c) and the cryoprobe is ready for operation.

Cryoprobe B (Figure 2) is the same as cryoprobe A except that the thermal insulation shell is connected rigidly to the cryoneedle. Thus, its outer diameter can be smaller than that of cryoprobe A.

Figure 3 is a schematic drawing of the LN_2 supply system. The LN_2 is contained under pressure in a 1.9-L vacuum-insulated container **(11)** (Brymill Co.). The LN_2 container is pressurized by compressed air from a low-pressure 34-L air tank **(15)**, through a flexible air-pressure pipe **(13)** and valve **(14)**. The low-pressure air tank is pre-charged with compressed air by an external pressure source. Experimental evidence indicates that a low pressure of 30 psi is satisfactory for the operation of the apparatus with three to five cryoprobes as described above. The volume of the low-pressure air tank is designed to be much larger than that of the LN_2 container. Therefore, the changes in total air volume during the entire cryosurgical operation are relatively small and are determined by the ratio of the volume of the LN_2 container to the volume of the low-pressure air tank. The pressure decrease in the low-pressure air tank is compensated by the pressure in the 22-L (120 psi) high-pressure air tank **(20)**. Pressure regulator **(18)** keeps the pressure in the low-pressure air tank at a set point (30 psi). The high-pressure air tank is needed only when successive cyrosurgical operations are being done. Some LN_2 boiling does take

LEGEND FOR FIGURES 1–4

1 Cryoneedle	13 Air pressure pipe
2 Thermocouple	14 Valve
3 Thermocouple wires	15 Low-pressure air tank
4 Thermal insulation shell	16 —
5 —	17 Pressure gauge
6 Protective tube	18 Pressure regulator
7 Flexible outlet tube	19 High pressure pipe
8 Fitting	20 High-pressure air tank
9 Feeding tube	21 —
10 LN_2 control valve	22 Temperature-measurement unit
11 Vacuum-insulated container	23 Thermocouple wires
12 —	24 Bleeding valve

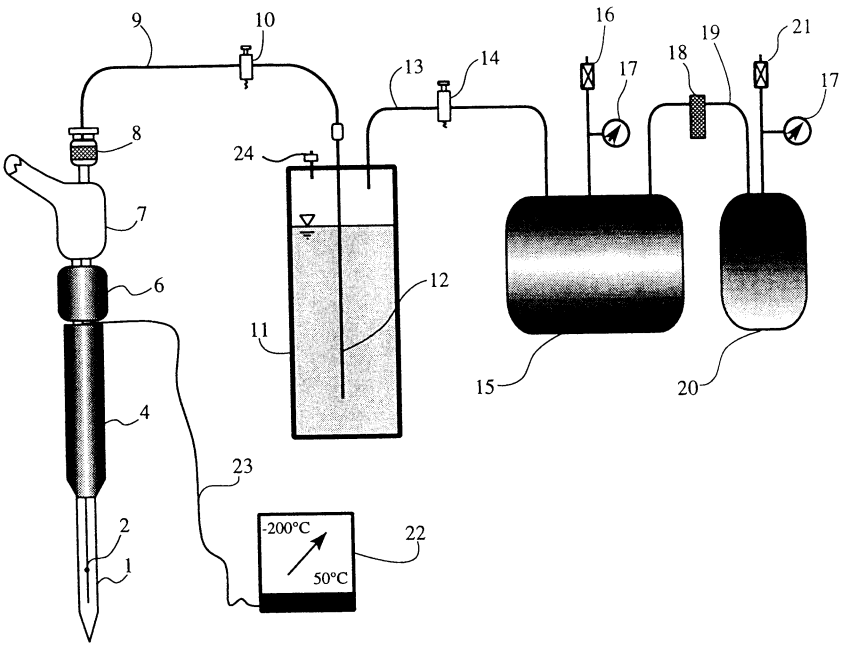

Figure 3. Schematic drawing of the pressurized liquid-nitrogen–supply system.

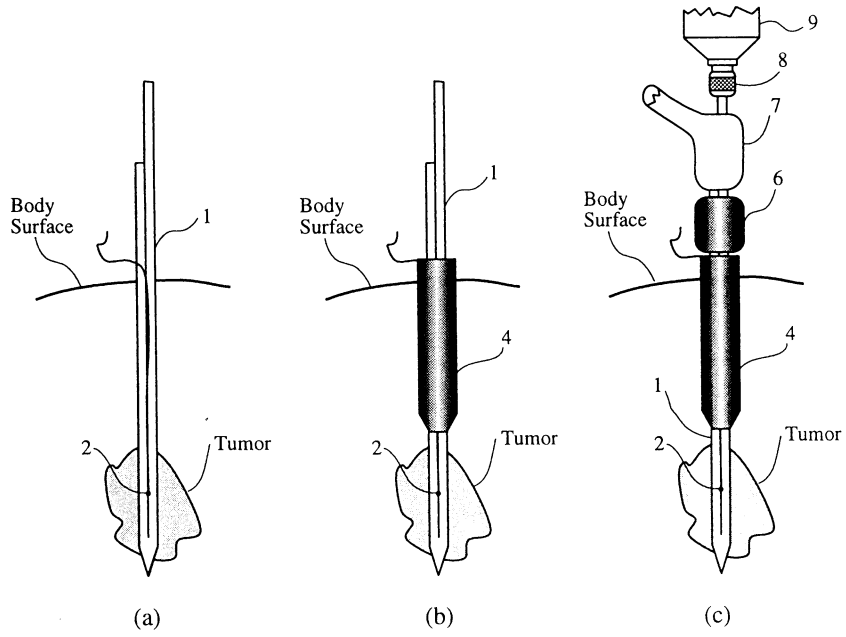

Figure 4. Schematic drawing of stages of cryoprobe insertion and localization: (a) insertion of the cryoneedle using an imaging device and a localization technique (such as ultrasonography or stereotaxis); (b) insertion of thermal insulation shell; (c) completion of the cryoprobe assembly and connection to a pressurized cryofluid source.

place within the LN_2 container; therefore, a bleeding valve (**24**), set at 30 psi, on the container compensates coolant volume changes while the system is in a standby condition. Any ordinary air compressor can serve as an air-pressure source for the LN_2 system. However, the air-pressure system described above has advantages as a part of a surgical apparatus in that it can be very light in weight, small in dimension, very quiet in operation, and independent in power supply.

Feeding tube (**9**) should be as short as possible, and therefore the LN_2 container should be placed as close as possible to the cryotreated tissue (the patient). This arrangement decreases the heat losses along the feeding tube to the surroundings, which decreases the required cryofluid flow rate, and which in turn decreases the volume of LN_2 container needed for a specific operation. In turn, a smaller LN_2 container requires a smaller air-tank volume. Low flow rates and a short feeding tube require lower working pressures in the air-pressure system. Therefore, the closer the LN_2 container is to the cryotreated tissues, the more compact in dimension and safer to use, in terms of pressure, the apparatus becomes.

METHODS

Pilot experiments were performed to demonstrate the effectiveness and the thermal efficiency of the experimental apparatus and the new cryoprobes. The apparatus and cryoprobes were tested first in gelatin solution (1.4%) and next in vivo, in the liver and thigh of a pig.

Two cryoprobe types were tested. The first type consisted of an uninsulated cryoneedle, to demonstrate the maximal cooling effect of the new cryoprobe configuration (cryoprobe A). The second type consisted of an insulated cryoneedle with the thermal insulation rigidly connected to the cryoneedle (cryoprobe B).

In the gelatin solution, the frozen-region dimensions were measured using photographs and an immersed measuring rod. Pictures where taken perpendicular to the center line of the cryoprobe. The immersed measuring rod was placed along the center line of the cryoprobe and below the cryoprobe tip. The frozen-region dimensions were measured by a ruler from the enlarged photographs, with reference to the measuring rod. The frozen region is always a cylindrical shape at the beginning of the freezing process, turning to an egg shape at a later stage, especially when short cryoneedles are used. Experimental results the maximal diameters of the frozen region are presented by Figure 5. The particular cryoprobe configurations, dimensions, and freezing media used in the experiments are presented by Table 1. The cryoprobe tip in experiment C2 was located 75 mm from the surface of the gelatin solution.

The cryoprobes were further tested in a three-cryoprobe configuration in gelatin solution. Figure 6 illustrates the freezing front location achieved with a three-cryoprobe operation, as viewed from above, parallel to the cryoprobes' center lines. Three identical thermal-insulated cryoprobes, similar to the one used in experiment C2, were used. A schematic drawing of the probe appears at the top left of Figure 6. The cryoprobes were

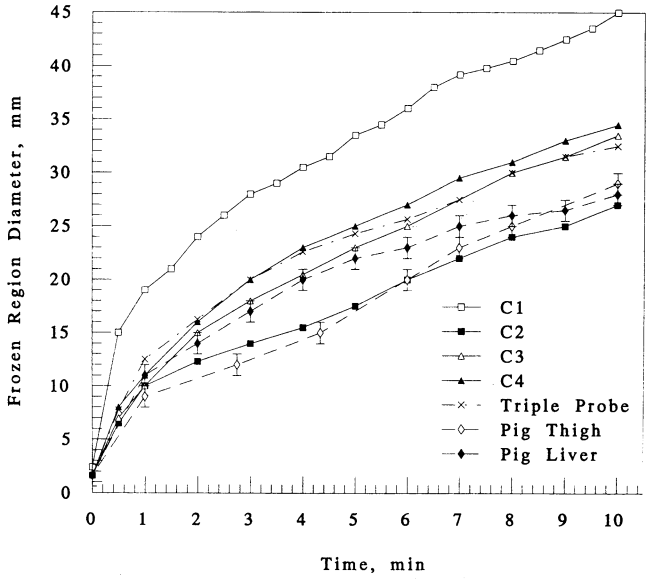

Figure 5. Maximal frozen-region diameters in gelatin solutions and in pig thigh and liver with selected cryoprobes. Particulars of these experiments are presented in Table 1. C1–C4 indicate experiments 1–4.

located 16.8 ± 0.3 mm distant from one another, at the heads of an imaginary triangle (represented by two black circles in Figure 6). The interface locations in Figure 6 are marked by numbers that represent the times from the beginning of the operation in minutes. Only the distances R1 and R2 were measured accurately during the operation, while the other data were interpolated from photographs, to provide a two-dimensional view of the process. Also note that, for considerations of symmetry, only one-third of the freezing surface is shown in Figure 6.

Following the work in gelatin solution, pilot in-vivo experiments were performed. These experiments were performed in the Surgical Oncology Laboratory at Al-

Table 1. Configuration and dimensions of the cryoprobes used for the experiments represented Figure 5

		Active Surface Length (mm)	Cryoneedle Tube Diameter (mm)	Thermal Insulation
Gelatin				
Experiment 1	(C1)	47	2.4 (13-gauge)	No
Experiment 2	(C2)	47	1.6 (16-gauge)	Yes
Experiment 3	(C3)	47	1.6 (16-gauge)	No
Experiment 4	(C4)	25	1.6 (16-gauge)	No
Pig thigh		37	1.6 (16-gauge)	No
Pig liver		18	1.6 (16-gauge)	No

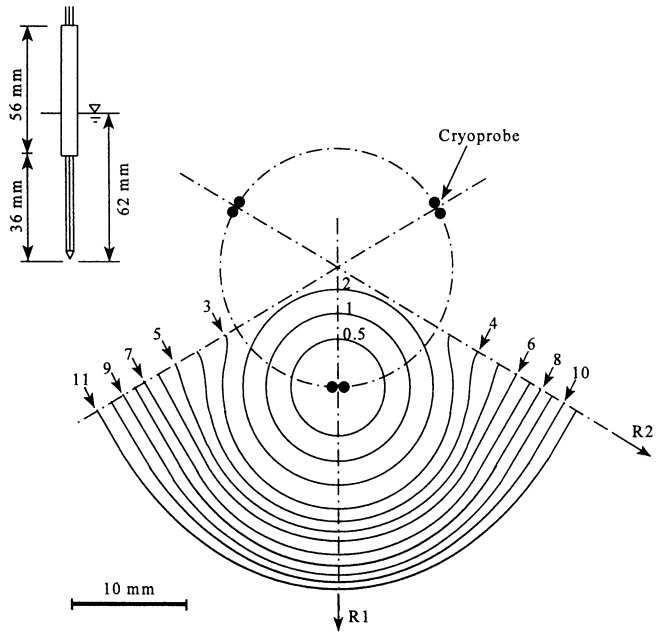

Figure 6. Two-dimensional view of the freezing front location in a three-cryoprobe operation. The numbers represent times in minutes from the beginning of the operation.

legheny General Hospital. These cryoprocedures were carried out in accordance with the guidelines and standards of the United States Public Health Services for use and care of laboratory animals and with the approval of the Institutional Animal Care and Use Committee of the Allegheny–Singer Research Institute. Three pilot experiments were performed to demonstrate the effectiveness of the new cryosurgical apparatus in perfused tissues, using a porcine model under general anesthesia. Cryoprobes were placed on the inner side of each hind thigh and into the liver of a pig weighing 34 kg. The cryoprobes used for the thighs were the same as the ones used for the gelatin experiments. The uninsulated cryoneedle was inserted to a depth of 37 mm after a 3-mm cut was made in the skin. The insulated cryoprobe, which has an active surface length of 36 mm, was inserted to a depth of 53 mm. All in-vivo experiments were terminated after 10 minutes of freezing.

After the above procedures had been carried out, the animal's abdomen was opened and the liver exposed. An uninsulated cryoneedle was inserted into the liver at the thickest section, to a depth of 18 mm. The animal was sacrificed about 15 minutes after completion of thawing at the end of the cryotreatment. Sacrifice was performed by standard protocol. A section of the liver within a 2–3-cm radius of the center of the cryoprobe was removed. The tissue was rapidly immersed in 10% natural buffered formaldehyde and stored for four days. It was then sectioned along the original tract of the cryoprobe. The thawed area was measured and tissue samples were taken for further histologic observations.

RESULTS AND DISCUSSION

It can be seen from Figure 5 that, regardless of the cryoneedle's active surface length, its diameter, or the presence of thermal insulation, the frozen region's diameter grew relatively rapidly in the first minute of operation, and that it was almost linearly time-dependent thereafter. It can also be seen that after 10 minutes of operation the frozen region's size was far from a steady-state condition. For the cryoneedle-tube diameter of 1.6 mm, the frozen regions' diameters ranged from 17.5 to 25 mm after 5 minutes of operation, and from 25 and 35 mm after 10 minutes of operation. It can be seen that the actual length of the frozen region is greater than the length of the cryoneedle's active surface, and therefore the diameter of the frozen region represents its smaller dimension. The actual length of the frozen region is about the length of the cryoneedle's active surface plus the radius of the frozen region for the uninsulated cryoneedle or the diameter of the frozen region for the insulated cryoneedle. As can further be seen, the diameter of the frozen region grows faster for a shorter cryoneedle.

A significant difference in the frozen-region diameters was found between experiment C1 and all other experiments, due to the use of larger tubes, 2.4 mm in diameter, in experiment C1. The cryoprobes are made of copper tubes, which typically have thick walls. The internal diameter of the tubes is the most important determinant of the LN_2 flow rate under a constant pressure for a given system. Assuming a highly turbulent flow in the tubes, it can be shown that the mass flow rate equals the product of some constant of the system and the inner diameter of the tube to the power of 2.5. Therefore, the flow rate in experiment C1 (2.4 mm tube with ID of 1.7 mm would be expected to be almost five times higher than that in experiment C3 (1.6 mm tube with ID of 0.9 mm). However, the ratio of the frozen-region volume of experiment C1 to that of experiment C3 is only about 2, which indicates that the usage of the thinner tube is much more thermal-efficient.

Freezing of biologic tissues is expected to require a higher cooling power, since perfusion of blood and metabolic activities produce heat and interfere with the cooling process. From Figure 5 it can be seen that the freezing front velocity in the liver diminished with time, while in the other experiments the velocities were almost linearly dependent on time (up to 10 minutes).

This may be explained by the large amount of blood perfusing the liver, which affects the freezing process.

It can be seen in Figure 6 that the freezing front propagation around each of the three cryoprobes is slower than that of a single cryoprobe (Figure 5). The frozen region became almost circular in cross section, with an average diameter of about 50 mm, after 11 minutes of operation. The length of the frozen region, parallel to the cryoprobes' center lines, was 42 mm after 2 minutes; it was 54 mm after 4 minutes, and 75 mm after 11 minutes.

The thermal efficiency of the cryosurgical device is defined in this study as the volume ratio of the frozen water to the volume of water that could have been frozen had all the heat sink generated by the boiling LN_2 been applied to the water. The water latent heat of freezing consumes most of the cooling power applied to the water, and the LN_2 latent heat of boiling produces almost all the cooling power. Therefore, thermal efficiency equals the product of the water latent heat (331.7 MJ/m^3) and the frozen-region volume, divided by the product of the LN_2 latent heat (199 MJ/m^3) and the volume of LN_2 used for the same operation.

The volume of the frozen region in the three-cryoprobe experiment was found to be 270 mL after 13 minutes of operation, by immersing the frozen gelatin in cold water and measuring the volume change of the water. The LN_2 consumption for the same 13 minutes of operation was 1,050 mL. Thus, the efficiency of the cryosurgical apparatus, in this particular operation, was 43%. The apparatus has a very short cryoprobe feeding line, which results in very small thermal heat losses, which in turn results in the high thermal efficiency. Cryodevice efficiency has not been previously reported in terms of liquid nitrogen consumption, but we consider this to be an important feature.

The diameters of the frozen regions as measured on the skin in the thigh experiment and on the liver surface in the liver experiment are shown in Figure 5. The thermophysical properties of skin differ from those of the underlying skeletal muscle, and the freezing front can be expected to propagate at different velocities in the different tissues. However, good agreement was found between frozen-region diameters on the skin surface and the diameters of the thawed cryoinjured regions. (The data for the insulated cryoprobe are not shown in Figure 5, since the frozen-region diameter on the skin does not correlate with the maximal frozen-region diameter in the muscles.) The skin surface that was in direct contact with the thermal insulation became frozen during the operation, however, and the freezing front propagated significantly more slowly in comparison with the areas of contact with the uninsulated cryoneedle. Histologic preparations were used to measure the dimensions of cryo-injured region. They revealed that cryoinjury was less severe around the thermal insulation than around the active surface of the cryoprobe. For the uninsulated probe in the thigh experiment, the primary cryo-injured region was in the muscles in a cylindrical configuration, having a diameter of 22 mm and a length of 48 mm. A partly-destroyed region surrounded the main cryo-injured region in a cylindrical shell shape was observed, having a thickness of 4–5 mm. An egg-shaped primary cryo-injured region was observed in the insulated-cryoprobe experiment, having a maximal diameter of 25 mm; a partly-destroyed region had a thickness of 3–4 mm. The skin, in both thigh experiments, thickened and deformed during the fixation procedure. The cryoprobe's original position was difficult to trace in the tissue, since cryoprobe penetration caused almost no damage.

The overall cross-sectional area of the cryoprobe is the most important design parameter for a minimally invasive procedure. Using thin-wall stainless steel tubes instead of the standard copper tubes used in the current study would maintain cryoprobe performance while reducing overall cross-sectional area. For example, a 1.6-mm (16-gauge) copper tube has the same inner diameter as a 1.1-mm (19-gauge) thin-wall stainless steel tube, and a 2.4-mm (13-gauge) copper tube has the same inner diameter as a 1.9-mm (about 14.5-gauge) thin-wall stainless steel tube. ■

The authors thank Dr. Peter Olson from the Department of Laboratory Medicine/Pathology at Allegheny General Hospital for the histologic analyses.

REFERENCES

1. *Orpwood RD. Biophysical and engineering aspects of cryosurgery. Phys Med Biol. 1981;26:555–75.*
2. *Rubinsky B, Onik G. Cryosurgery: advances in the application of low temperature to medicine. Int J Refrig. 1991:14:1–10.*
3. *Gage AA. Current progress in cryosurgery. Cryobiology. 1988;25:483–6.*
4. *Gage AA. Progress in cryosurgery. Cryobiology. 1992;29:300–4.*
5. *Gao XK, Sun DK, Sha RJ, Ding YS, Yan QY, Zhu CD. Precooled, spring-driven surgical cryoneedle: a new device for cryohaemorrhoidectomy. Proceedings of the 11th International Cryogenic Engineering Conference, IECE 11, Berlin, West Germany. 1986;825–9.*
6. *Kollner P, Duczek, E. Apparatus for cryosurgery. U.S. Patent No. 3,794,039. 1974.*

7. *Timmerhause KD. Trends to miniature cryogenic refrigeration systems and components. Int J Refrig. 1989;12:246–54.*
8. *Hamilton A, Hu J. An electronic cryoprobe for cryosurgery using heat pipes and thermoelectric coolers: a preliminary report. J Med Eng Technol. 1993;17(3):104–9.*
9. *Weshahy AH. Interlesional cryosurgery: a new technique using cryoneedles. J Dermatol Surg Oncol. 1993;19:123–6.*
10. *Rzasa RP, Wallach RM. Cryosurgical instrument. U.S. Patent No. 4,377,168. 1983.*
11. *Homasson JP, Thiery JP, Angebault M, Ovtracht L, Maiwand O. The operation and efficacy of cryosurgical, nitrous oxide-driven cryoprobe. Cryobiology. 1994;31:290–304.*
12. *Cooper IS, Lee A. Cryostatic congelation: a system for producing a limited controlled region of cooling or freezing of biological tissues. J Nerv Ment Dis. 1961;133:259–63.*
13. *Chang Z, Finkelstein JJ, Ma H, Baust J. Development of a high-performance multiprobe cryosurgical device. Biomed Instrum Technol. 1994;28:383–90.*
14. *Rabin Y, Shitzer A. A new cryosurgical device for controlled freezing. Part I: setup and validation test. Cryobiology. 1996;33:82–92.*
15. *Onik G, Gilbert J, Hoddick W, et al. Sonographic monitoring of hepatic cryosurgery in an experimental animal model. AJR Am J Roentgenol. 1985;144:1043–7.*
16. *Onik G, Rubinsky B, Zemel R, et al. Ultrasound-guided hepatic cryosurgery in the treatment of metastatic colon carcinoma—preliminary results. Cancer. 1991;67:901–7.*
17. *Isoda H. Sequential MRI and CT monitoring in cryosurgery—an experimental study in rats [in Japanese]. Nippon Igaku Hoshasen Gakkai Zasshi. Nippon Acta Radiol. 1989;49:1499–508.*
18. *Gilbert JC, Rubinsky B, Roos MS, Wong STS, Brennan KM. MRI-monitored cryosurgery in the rabbit brain. Magnetic Resonance Imaging. 1993;11:1155–64.*
19. *Rubinsky B, Gilbert JC, Onik GM, Roos MS, Wong STS, Brennan KM. Monitoring cryosurgery in the brain and the prostate with proton NMR. Cryobiology. 1993;30:191–9.*
20. *Smith JJ, Fraser J. An estimation of tissue damage and thermal history in cryolesions. Cryobiology. 1974;11:139–47.*
21. *Gage AA, Guest K, Montes M, Garuna JA, Whalen DA Jr. Effect of varying freezing and thawing rates in experimental cryosurgery. Cryobiology. 1985;22:175–82.*
22. *Rabin Y, Coleman R, Mordohovich D, Ber R, Shitzer A. A new cryosurgical device for controlled freezing. Part II: in vivo experiments on rabbits' skeletal muscle hindlimb. Cryobiology. 1996;33:93–105.*
23. *Miller RH, Mazur P. Survival of frozen-thawed human red cells as a function of cooling and warming velocities. Cryobiology. 1976;13:404–14.*
24. *Rand RW, Rand RP, Eggerding FA, et al. Cryolumpectomy for breast cancer: an experimental study. Cryobiology. 1985;22:307–18.*